THE JOURNAL OF BIOLOGICAL CHEMISTRY VOL. 285, NO. 23, pp. 17310–17317, June 4, 2010

A Novel Intronic Peroxisome Proliferator-activated Receptor γ Enhancer in the Uncoupling Protein (UCP) 3 Gene as a Regulator of Both UCP2 and -3 Expression in Adipocytes*

Received for publication, March 8, 2010, and in revised form, March 22, 2010 Published, JBC Papers in Press, April 1, 2010, DOI 10.1074/jbc.M110.120584

Anne Bugge[‡1], **Majken Siersbæk**[‡1], **Maria S. Madsen**[‡2], **Anita Göndör**[§], **Carole Rougier**[¶], **and Susanne Mandrup**[‡3]

From the [‡]*Department of Biochemistry and Molecular Biology, University of Southern Denmark, Campusvej 55, 5230 Odense M, Denmark, the* [§]*Department of Microbiology, Tumor and Cell Biology, Karolinska Institute, Stockholm SE-171 77, Sweden, and the* [¶]*Department of Development and Genetics, Uppsala University, Uppsala SE-751 05, Sweden*

Uncoupling Proteins (UCPs) are integral ion channels residing in the inner mitochondrial membrane. UCP2 is ubiquitously expressed, while UCP3 is found primarily in muscles and adipose tissue. Although the exact molecular mechanism of action is controversial, it is generally agreed that both homologues function to facilitate mitochondrial fatty acid oxidation. UCP2 and -3 expression is activated by the peroxisome proliferator-activated receptors (PPARs), but so far no PPAR response element has been reported in the vicinity of the *Ucp2* and *Ucp3* genes. Using genome-wide profiling of PPARγ occupancy in 3T3-L1 adipocytes we demonstrate that PPARγ associates with three chromosomal regions in the vicinity of the *Ucp3* locus and weakly with a site in intron 1 of the *Ucp2* gene. These sites are isolated from the nearest neighboring sites by >900 kb. The most prominent PPARγ binding site in the *Ucp2* and *Ucp3* loci is located in intron 1 of the *Ucp3* gene and is the only site that facilitates PPARγ transactivation of a heterologous promoter. This site furthermore transactivates the endogenous *Ucp3* promoter, and using chromatin conformation capture we show that it loops out to specifically interact with the *Ucp2* promoter and intron 1. Our data indicate that PPARγ transactivation of both UCP2 and -3 is mediated through this novel enhancer in *Ucp3* intron 1.

Uncoupling proteins (UCPs)[4] are integral ion-channels residing in the inner mitochondrial membrane. The founding member of the family, UCP1, is exclusively expressed in brown adipose tissue, where it plays a central role in adaptive thermogenesis (1). UCP1 uncouples the oxidation of metabolic intermediates from the generation of ATP by dissipating the proton gradient thereby releasing the energy as heat (2). Several UCP1 homologues have been discovered, including UCP2 and UCP3, which share 59 and 57% amino acid identity with UCP1, respectively (3, 4). The genes encoding these two UCP isoforms are located head to tail on chromosome 7 in mice (chromosome 11 in humans) and separated by ~20 kb. UCP2 is expressed in several tissues, including lung, kidney, pancreas, and white adipose tissue, whereas UCP3 is expressed primarily in muscle and in brown and white adipose tissue (3, 4). Although reconstitution and overexpression experiments have demonstrated that UCP2 and UCP3 can function as proton channels (3, 5, 6), UCP2 (7) and UCP3 (8, 9) knock-out mice maintain normal body temperature during cold exposure. Thus, UCP2 and UCP3 do not appear to contribute significantly to cold-induced thermogenesis in mice, and it has been contested whether UCP2 and UCP3 display uncoupling activity *in vivo*. Interestingly, a number of other studies have suggested that the primary function of UCP2 and UCP3 is to limit the production of reactive oxygen species associated with respiration (7, 10). Indeed, reactive oxygen species production is elevated in UCP2 null mice (11), which is reflected in the increased microbicidal activity of macrophages isolated from these animals (7). Other widely held hypotheses consider UCP3 to function to limit oxidation of pyruvate (10) or to be an exporter of the toxic fatty acid anions and peroxides that accumulate in the mitochondria during periods of elevated β-oxidation (12). Consistent with this hypothesis, muscle UCP3 levels are increased by fasting (13) and intralipid infusion (14). However, it is controversial whether the UCP3 knock-out mice display normal (9) or reduced fatty acid oxidation rates (14). Although a recent study rejects the hypothesis of UCP3 being a fatty acid anion exporter, there is a consensus that lack of UCP3 does lead to a decrease in the mitochondrial fatty acid oxidation capacity during fasting (15).

Several studies have indicated that the peroxisome proliferator-activated receptor (PPAR) transcription factor family regulates both UCP2 and UCP3 expression. The PPARα (16, 17) and PPARβ/δ (18–20) subtypes activate genes involved in lipid oxidation (21, 22), and they target UCP2 and -3 in liver and muscles, respectively. The PPARγ subtype activates both lipogenic and lipid oxidation genes (23, 24) and is highly expressed in adipocytes, where it is a master regulator of adipogenesis (25). UCP3 mRNA is increased in the white adipose tissue of rodents fed a PPARγ agonist (26, 27), and induction of both UCP2 and

* This work has been supported in part by grants from the Danish Natural Science Research Foundation, the Novo Nordisk Foundation, and grants from NordForsk given to the Nordic Center of Excellence MitoHealth.

[1] Both authors contributed equally to this work.

[2] Supported by the Novo Scholarship program.

[3] To whom correspondence should be addressed: Dept. of Biochemistry and Molecular Biology, University of Southern Denmark, Campusvej 55, 5230 Odense M, Denmark. Tel.: 45-6550-2340; Fax: 45-6550-2467; E-mail: s.mandrup@bmb.sdu.dkmailto.

[4] The abbreviations used are: UCP, uncoupling protein; PPAR, peroxisome proliferator-activated receptor; RXR, retinoid X receptor; PPRE, PPAR response element; ChIP, chromatin immunoprecipitation; ChIP-seq, ChIP sequencing; 3C, chromatin conformation capture; HA, hemagglutinin; CMV, cytomegalovirus.

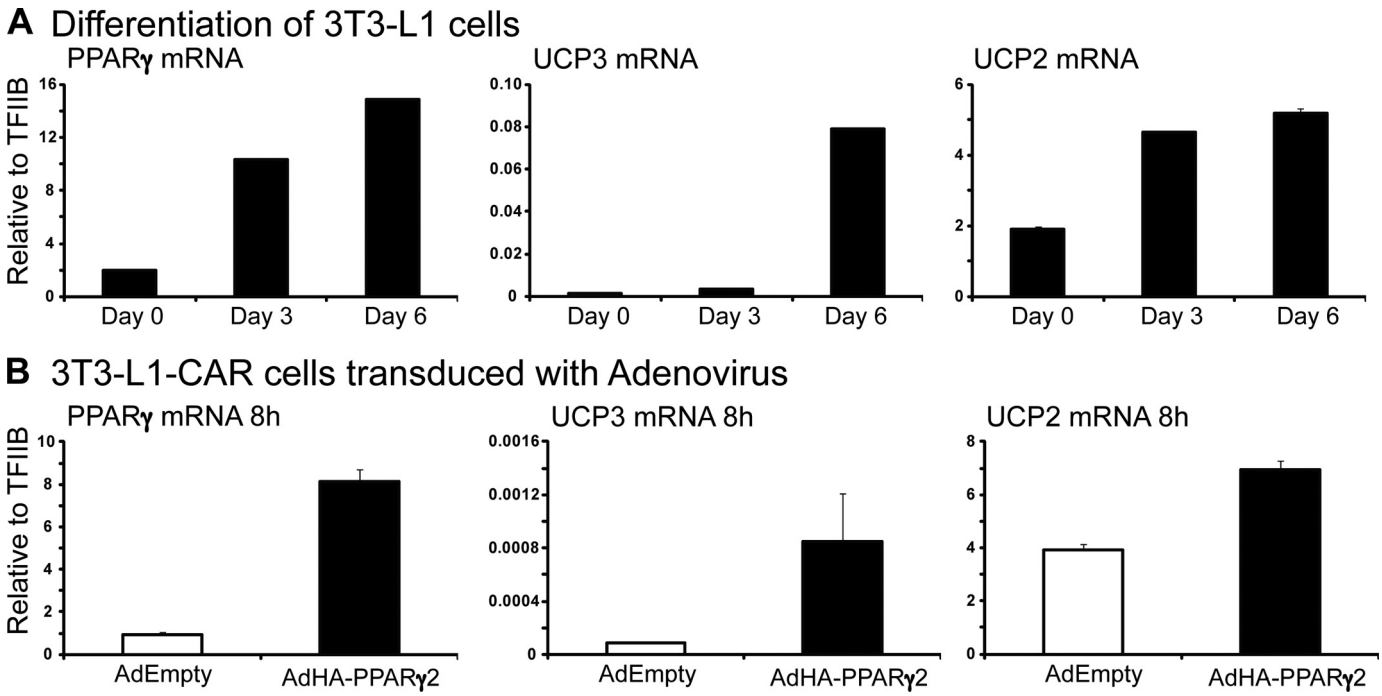

FIGURE 1. **UCP2 and -3 are target genes of PPARγ in 3T3-L1 cells.** *A*, mRNA expression of PPARγ, UCP3, and UCP2 during 3T3-L1 adipogenesis. Levels of mRNA was determined by real-time PCR and normalized to the corresponding TFIIB levels. The experiment was performed in duplicate, and the range is indicated. This experiment is representative of three individual experiments. *B*, ectopic expression of PPARγ2 in 3T3-L1 preadipocytes induces UCP2 and -3 mRNA expression. 3T3-L1- CAR preadipocytes were transduced with adenovirus expressing PPARγ2 (*AdHA-PPARγ2*) in the presence of 1 μM PPARγ agonist rosiglitazone, or with control adenovirus containing empty vector (*AdEmpty*) in the presence of vehicle (DMSO). Total RNA was harvested 8 h after transduction, and the mRNA expression of PPARγ, UCP3, and UCP2 was determined by real-time PCR and normalized to the corresponding TFIIB levels. The experiment was performed in triplicate, and the range is indicated.

-3 expression has been demonstrated in clonal adipocyte cell lines and isolated adipocytes (28–30).

The PPARs bind direct repeats of 5′-AGGTCA-3′ spaced by one nucleotide (DR1) as obligate heterodimers with the retinoid X receptors (RXRs) (31, 32). However, so far no such PPAR response elements (PPREs) have been annotated within or in vicinity of the *Ucp2* and *Ucp3* genes. Three potential PPREs have been indicated by *in silico* analysis of the human *UCP3* promoter, but it is unclear whether these are functional (33, 34). Furthermore, it was recently shown that in both humans and hamsters, specific regions or a single base pair in intron 1 are essential for expression of UCP3 in skeletal muscles (35) and brown adipose tissue (36), respectively. Interestingly, in hamsters, this single base polymorphism, which determines tissue-specific expression of UCP3, also confers responsiveness to PPAR agonists, although no PPRE was identified in the sequence of ~40 bp of genomic DNA centered on the polymorphism (36).

The PPAR-mediated regulation of UCP2 appears to be indirect, but has been reported to be dependent on a double E-box motif in the proximal promoter (37, 38). In addition, it has been demonstrated that the activity of UCP2 is regulated by two silencer elements, one of which is located in intron 1 (38).

We have previously described an intronic PPRE (39), and using genome-wide chromatin immunoprecipitation sequencing (ChIP-seq) profiling we have shown that 47% of all PPARγ/RXR binding sites in 3T3-L1 cells are found in intronic regions (40). Here we show that intron 1 of the murine *Ucp3* gene contains such a PPARγ/RXR binding site, centered on a DR1 element that enables PPARγ activation of reporter constructs in transient transfections. Using the chromatin conformation capture (3C) technique we demonstrate that the PPARγ/RXR binding site in intron 1 of *Ucp3* loops out to interact specifically with the promoter and 5′-region of *Ucp2*, in 3T3-L1 adipocytes suggesting that PPARγ transactivation of both UCP2 and -3 is mediated through the binding site in *Ucp3* intron 1.

EXPERIMENTAL PROCEDURES

Retroviral Transduction of 3T3-L1 Cells—Phoenix cells were transfected using the calcium phosphate technique with a retroviral LXSN-hCARΔ1 vector expressing the truncated coxsackie-adenovirus receptor (CARΔ1) (41) at 50% confluence. Two days after transfection, virus supernatant was harvested and centrifuged to remove phoenix cells. To generate 3T3-L1-CAR cells, 3T3-L1 cells at 50% confluence were transduced with a 1:1 dilution of virus supernatant and fresh growth medium in the presence of 6 μg/ml Polybrene (Sigma-Aldrich) and subjected to neomycin (G418, 0.7 mg/ml, Bie and Berntsen) selection the following day.

Cell Cultures—3T3-L1 and 3T3-L1-CAR preadipocytes were cultured in Dulbecco's modified Eagle's medium (Invitrogen) supplemented with 10% calf serum (Fischer Scientific PAA). Phoenix and HEK293T cells were grown in Dulbecco's modified Eagle's medium supplemented with 10% fetal calf serum (Biochrom AG). All cell lines were kept in medium supplemented with streptomycin (100 μg/ml) and penicillin (62.5 μg/ml). The 3T3-L1 fibroblasts were differentiated to adipocytes by stimulation with 3-isobutyl-1-methylxanthine, dexamethasone, and insulin as described previously (39).

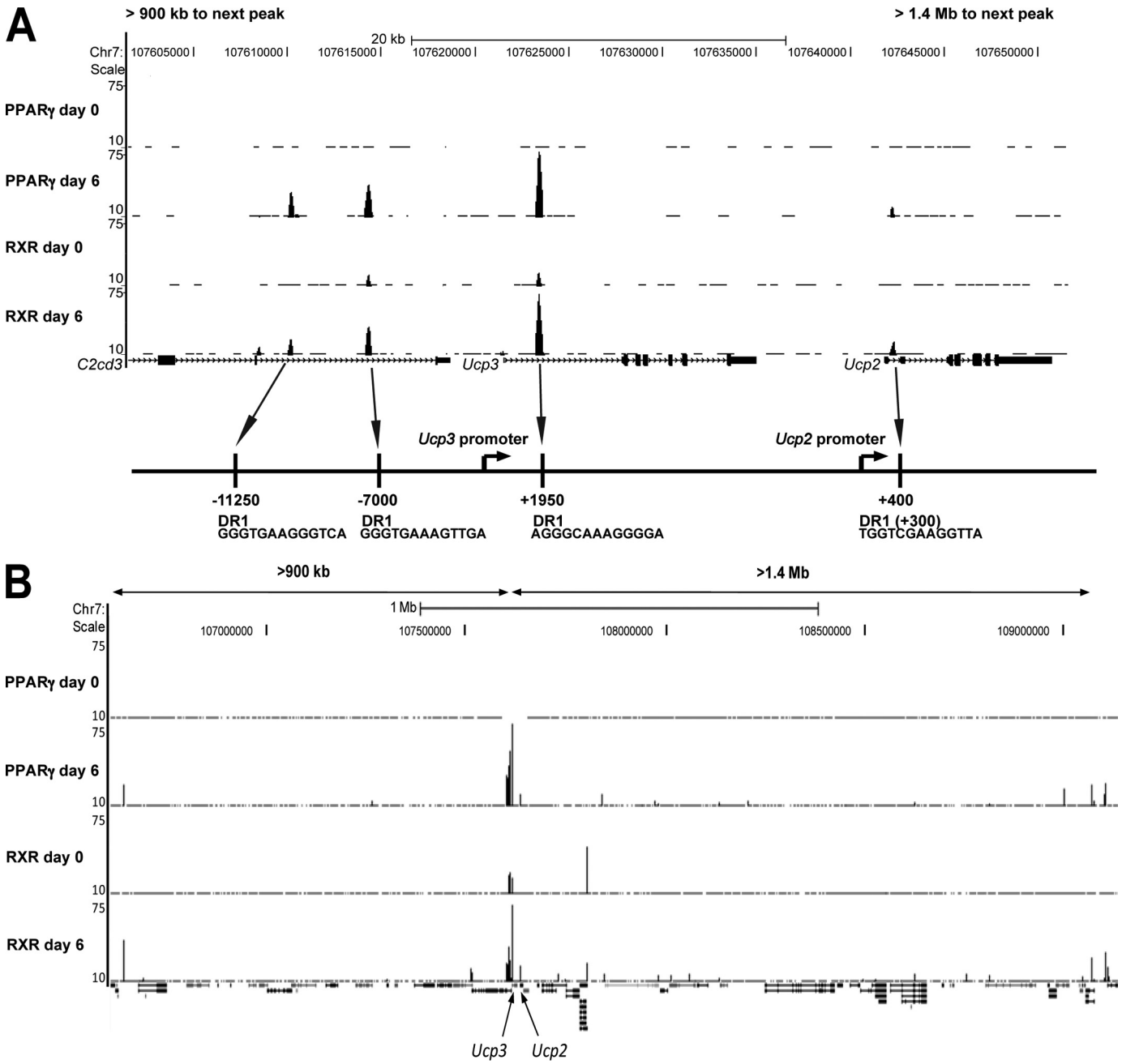

FIGURE 2. **PPARγ/RXR ChIP-seq profile of the *Ucp2* and *Ucp3* loci.** Screen shots from the genome-wide ChIP-seq profile of PPARγ/RXR binding sites in 3T3-L1 cells by Nielsen *et al.* (40) on days 0 and 6 of differentiation. *A*, *close-up* of the murine *Ucp2* and *-3* loci with a schematic representation indicating the positions of the PPARγ/RXR binding sites and DR1 elements relative to the transcription start sites shown below. *B*, overview of the PPARγ and RXR binding profiles on >2.3 Mb of chromosome 7 encompassing the *Ucp2* and *-3* genes. The genomic distances to the neighboring PPARγ/RXR binding sites relative to the sites in the *Ucp3* and *-2* locus are indicated.

Adenoviral Transduction—The generation of and transduction with adenovirus encoding HA-tagged mouse PPARγ2 was performed as previously described (23). Briefly, adenovirus was suspended in medium and added to 3T3-L1-CAR cells at 80% confluency. After 2 h of transduction, the virus-containing medium was removed and new medium containing the vehicle DMSO or 1 μM rosiglitazone (BRL49653) was added for an additional 6 h.

RNA Extraction and cDNA Synthesis—Cells were harvested in 500 μl of TRIzol™. Total RNA was extracted by addition of chloroform and precipitated with isopropanol and centrifugation. The pellet was washed with 75% ethanol and redissolved in diethyl pyrocarbonate-treated water. From each preparation, 1 μg of RNA was subjected to DNase I (Invitrogen) treatment, and cDNA was synthesized using random deoxynucleic acid hexamers and reverse transcriptase (First-Strand Kit, Invitrogen) as previously described (42).

Chromatin Immunoprecipitation—ChIP was performed as previously described (40). Antibodies used were anti-PPARγ (H-100, sc7196, Santa Cruz Biotechnologies, Santa Cruz, CA), and anti-RXR (Δ197, sc774, Santa Cruz Biotechnologies).

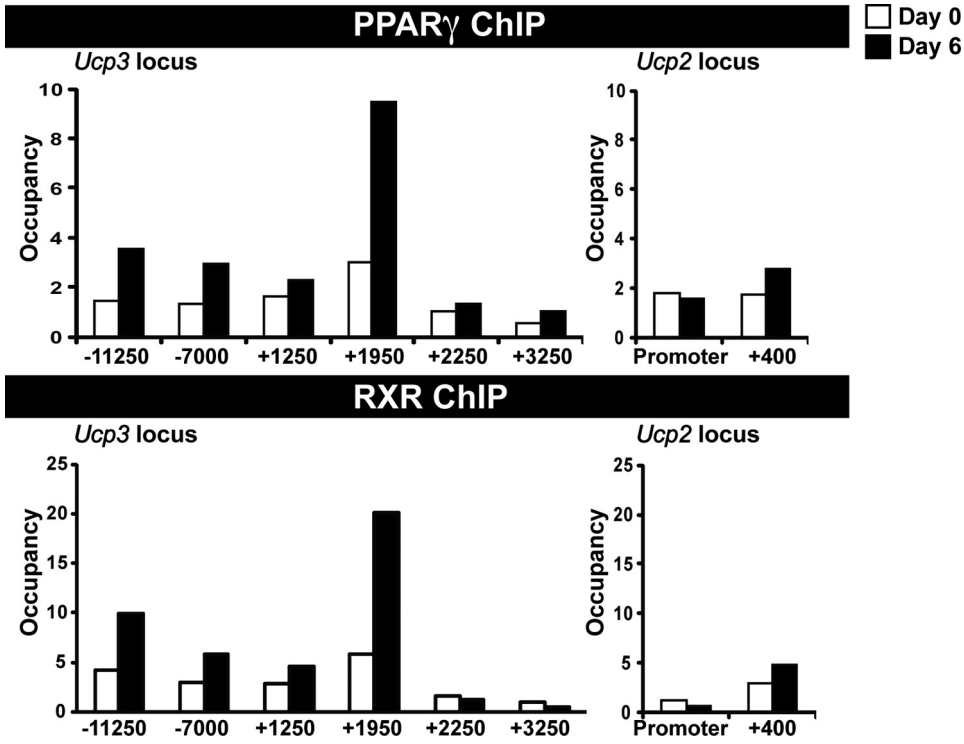

FIGURE 3. **PPARγ and RXR binding sites are found in proximity and within the *Ucp2* and *-3* genes.** PPARγ and RXR ChIP-PCR to confirm binding sites identified by ChIP-seq. Chromatin was harvested from cross-linked 3T3-L1 cells on days 0 and 6 of differentiation. ChIP was performed using antibodies against PPARγ or RXR. Occupancy (-fold enrichment above myoglobin promoter levels) at the binding sites found in Fig. 2 and at intermittent control regions was determined by real-time PCR. This experiment is representative of three independent experiments.

Real-time PCR—Quantitative three-step real-time PCR was performed on the Mx3000 real-time PCR instrument (Stratagene) using 2×SYBR Green Master Mix and Sigma passive reference (Sigma-Aldrich) according to the instructions from the manufacturer. All measurements were performed in duplicate. Primers for real-time PCR (sequences available upon request) were designed using Primer Express 2.0 (Applied Biosystems) or Primer3 (available on-line). Specificity and efficacy were validated before use.

Cloning and Sequencing—The PPARγ/RXR binding sites detected in proximity and within the murine *Ucp3* and *Ucp2* genes were PCR-cloned in front of the SV40 promoter in the pGL3-Promoter vector using primers generating MluI and XhoI (New England Biolabs) restriction sites. The *Ucp3* proximal promoter (~450 bp) and +1950 PPARγ/RXR binding site was PCR-cloned into the pGL3-Basic vector upstream and downstream of the luciferase gene, respectively, using primers generating MluI and XhoI (New England Biolabs) restriction sites. The DR1 element in the +1950 PPARγ/RXR binding site was subsequently mutated by the introduction of an ApaI (New England Biolabs) site. The 3C PCR product was cloned into pCR™ 4Blunt-TOPO™ by Zero Blunt™ TOPO™ PCR Cloning (Invitrogen). Sequencing was performed on the ABI prism 310 using the Big Dye Terminator v1.1, v3.1 Kit (Applied Biosystems).

Transient Transfections—HEK293T cells were transfected at 90% confluence with the pGL3 reporter constructs, pShuttle-CMV-PPARγ, and a pCMV-β-galactosidase (Promega, Madison, WI) control in 24-well plates using Metafectene Pro (Biontex). Following 5 h of incubation, the medium was exchanged to fresh medium containing DMSO or 1 μM rosiglitazone. Cells were harvested 19 h later in lysis buffer (Tropix) and luciferase, and β-galactosidase assays were performed as described previously (43). All experiments were performed in triplicate, and luciferase and β-galactosidase activities were measured in duplicate.

Chromatin Conformation Capture—Nuclei were isolated by 15-min incubation in 1 × TE buffer (1 mM EDTA, 10 mM Tris-HCl (pH 8.0)) supplemented with 0.5% Triton X-100 at 37 °C, followed by 15 min of centrifugation at 3000 rpm and 4 °C. The remaining preparation of the chromatin conformation capture (3C) samples and controls was performed as previously described (44) using the Csp6I restriction enzyme. Control fragments for the evaluation of 3C primers were generated by PCR amplification (Phusion hot start high-fidelity DNA polymerase, Finnzymes) of the regions flanking the Csp6I restriction sites at *Ucp3* intron 1, the 5′-end of *Ucp2*, and the regions upstream and downstream of the latter. The fragments were mixed in equimolar concentration, digested with Csp6I, purified using the Qiagen PCR purification kit, and ligated with T4 DNA ligase (New England Biolabs). Serial dilutions (2, 4, 8, and 16 fg per reaction) of these *in vitro*-generated templates were used to evaluate the specificity of the 3C primers (sequences available upon request) in a background of 50 ng of Csp6I-digested 3T3-L1 genomic DNA. Subsequently, PCR conditions were optimized to obtain comparable sensitivity and linear amplification for all primer sets.

RESULTS

UCP2 and UCP3 Expression Is Regulated by PPARγ in 3T3-L1 Cells—It has previously been demonstrated that UCP2 and UCP3 expression is rapidly up-regulated in adipocyte cell lines exposed to PPARγ agonists (28, 30), whereas the undifferentiated cells are unresponsive (30). Correspondingly, both UCP2 and UCP3 mRNA levels increased as the murine 3T3-L1 cells underwent adipogenesis (Fig. 1*A*). The increase is proportionally larger for UCP3, which is expressed at very low levels in undifferentiated 3T3-L1 cells, whereas the mRNA level of the highly expressed UCP2 is approximately doubled. To further establish that UCP2 and -3 are direct target genes of PPARγ, we transduced 3T3-L1-CAR cells (3T3-L1 cells ectopically expressing CARΔ1 to facilitate adenovirus uptake) with adenoviral vectors expressing HA-tagged mouse PPARγ2. We have previously shown that adenoviral expression of PPARγ2 leads to rapid

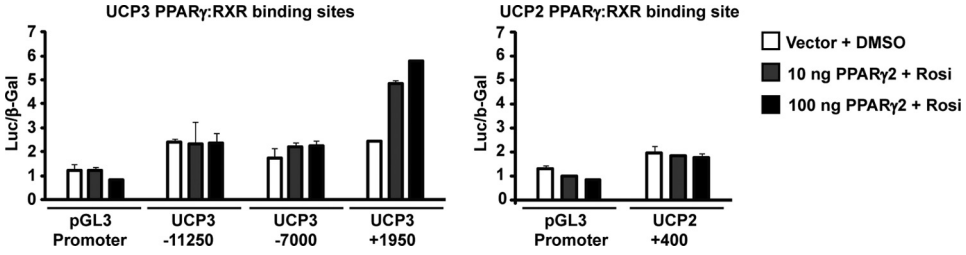

FIGURE 4. **Only the PPARγ/RXR binding site in intron 1 of the *Ucp3* gene mediates PPARγ transactivation of a heterologous promoter.** Approximately 500 bp surrounding the PPARγ/RXR binding sites in *Ucp2* and *-3* were cloned in front of a SV40 promoter in the pGL3-Promoter luciferase reporter vector and transfected into HEK293T cells together with increasing amounts of PPARγ2 expression vector in the presence of 1 μM rosiglitazone or the vehicle DMSO as indicated. Luciferase levels were normalized to the expression from a β-galactosidase control vector. Results are representative of three independent experiments, each performed in triplicate. Standard deviations are indicated.

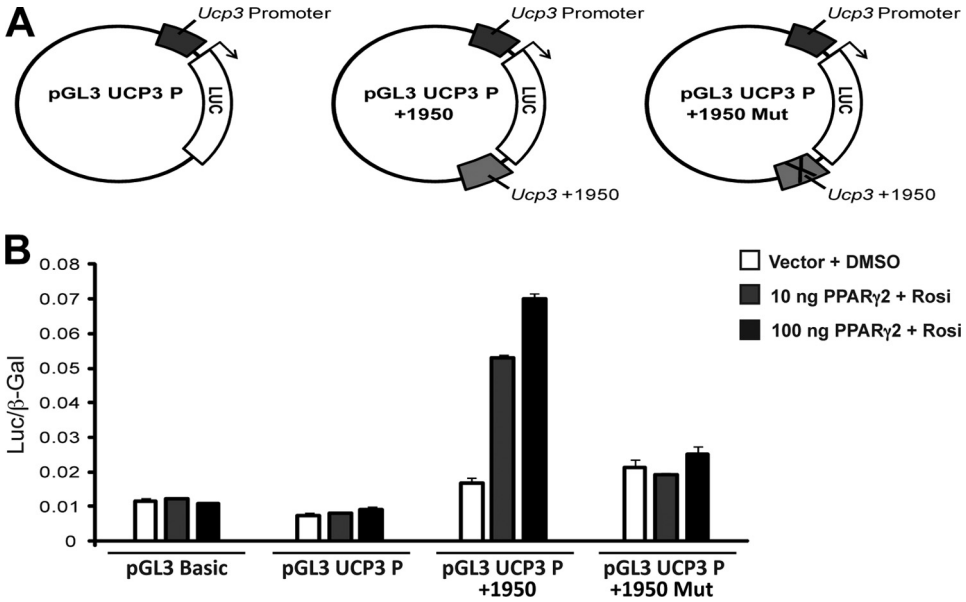

FIGURE 5. **The +1950 PPARγ/RXR binding site in the *Ucp3* gene enables PPARγ-transactivation of the endogenous *Ucp3* promoter.** *A*, the *Ucp3* proximal promoter (~450 bp) and the +1950 PPARγ/RXR binding site were cloned into the promoterless pGL3-Basic vector upstream and downstream of the luciferase gene, respectively. The DR1 element in the +1950 PPARγ/RXR binding site was subsequently mutated by the introduction of an ApaI site. *B*, transfections were performed as in Fig. 4. Results are representative of three independent experiments each performed in triplicates. Standard deviations are indicated.

establishment of transcriptionally active complexes, thus allowing us to evaluate the immediate effects on target gene activity at the mRNA level within 8 h post transduction (23). Subjecting the 3T3-L1-CAR preadipocytes to PPARγ2 adenovirus in combination with the potent PPARγ agonist rosiglitazone, led to an increase in UCP2 and UCP3 expression comparable to the levels induced by adipogenesis (Fig. 1*B*), thereby confirming that both UCP2 and UCP3 are primary targets of PPARγ in 3T3-L1 cells.

ChIP-seq Profiling Detects PPARγ Binding in the Vicinity and within the Ucp2 and -3 Loci—We recently used ChIP-seq to generate genome-wide maps of PPARγ and RXR binding sites throughout adipocyte differentiation of 3T3-L1 cells (40). Based on these data we identified prominent PPARγ/RXR peaks in the *Ucp3* locus at position −11250, −7000, and +1950 relative to the transcription start site. By contrast, the *Ucp2* locus and surroundings displayed only a single very low intensity peak at +400 relative to the transcription start site (Fig. 2*A*). These sites are >900 kb from the neighboring PPARγ binding sites (Fig. 2*B*). PPARγ and RXR binding was confirmed by ChIP-PCR (Fig. 3), which in accordance with the ChIP-Seq data showed highest occupancy at the +1950 binding site in *Ucp3*, and very low occupancy at the +400 binding site in *Ucp2*. This pattern of PPARγ/RXR binding was also found in the murine hepatoma cell line AML-12 upon adenoviral expression of PPARγ2 (unpublished ChIP-Seq results).

NHR-scan (available on-line) found degenerate DR1 elements in the genomic regions directly below the three binding sites in and near the *Ucp3*, and one in proximity of, although not positioned directly beneath, the binding site in *Ucp2* (Fig. 2*A*).

The Ucp3 + 1950 DR1 Element Enables PPARγ-mediated Transactivation of Reporter Constructs—PPARγ/RXR occupancy as detected in ChIP may be the result of direct binding to a PPRE or of indirect binding to DNA via other transcription factors. To evaluate which of the PPARγ/RXR binding sites found within and in the vicinity of the *Ucp2* and *Ucp3* loci could be potential PPREs, the DR1 elements and surrounding ~500 bp were cloned in front of the SV40 basal promoter in the pGL3 luciferase reporter construct. Interestingly, only the *Ucp3* + 1950 region mediated a dose-dependent increase in transcription of the luciferase reporter upon co-expression of PPARγ2 (Fig. 4). By contrast, neither the *Ucp3* −11250 or −7000 regions nor the *Ucp2* + 400 region conferred PPARγ responsiveness to these reporter constructs (Fig. 4).

As the intronic +1950 region of *Ucp3* clearly contains the most prominent and functional PPARγ/RXR binding site in the *Ucp3* and *-2* loci, we cloned the ~500-bp fragment encompassing this binding site into the promoter-less pGL3-Basic vector together with the proximal *Ucp3* promoter (~450 bp) immediately downstream and upstream of the luciferase gene, respectively (Fig. 5*A*). Again, the intronic *Ucp3* PPARγ/RXR binding site facilitated significantly enhanced dose-dependent luciferase activity in response to PPARγ overexpression. Importantly, this ability was critically dependent on the presence of the +1950 DR1 element, because PPARγ transactivation was abolished by mutation of this site (Fig. 5*B*). These results show that PPARγ transactivation of UCP3 primarily is mediated through the DR1 element at position +1950 in intron 1.

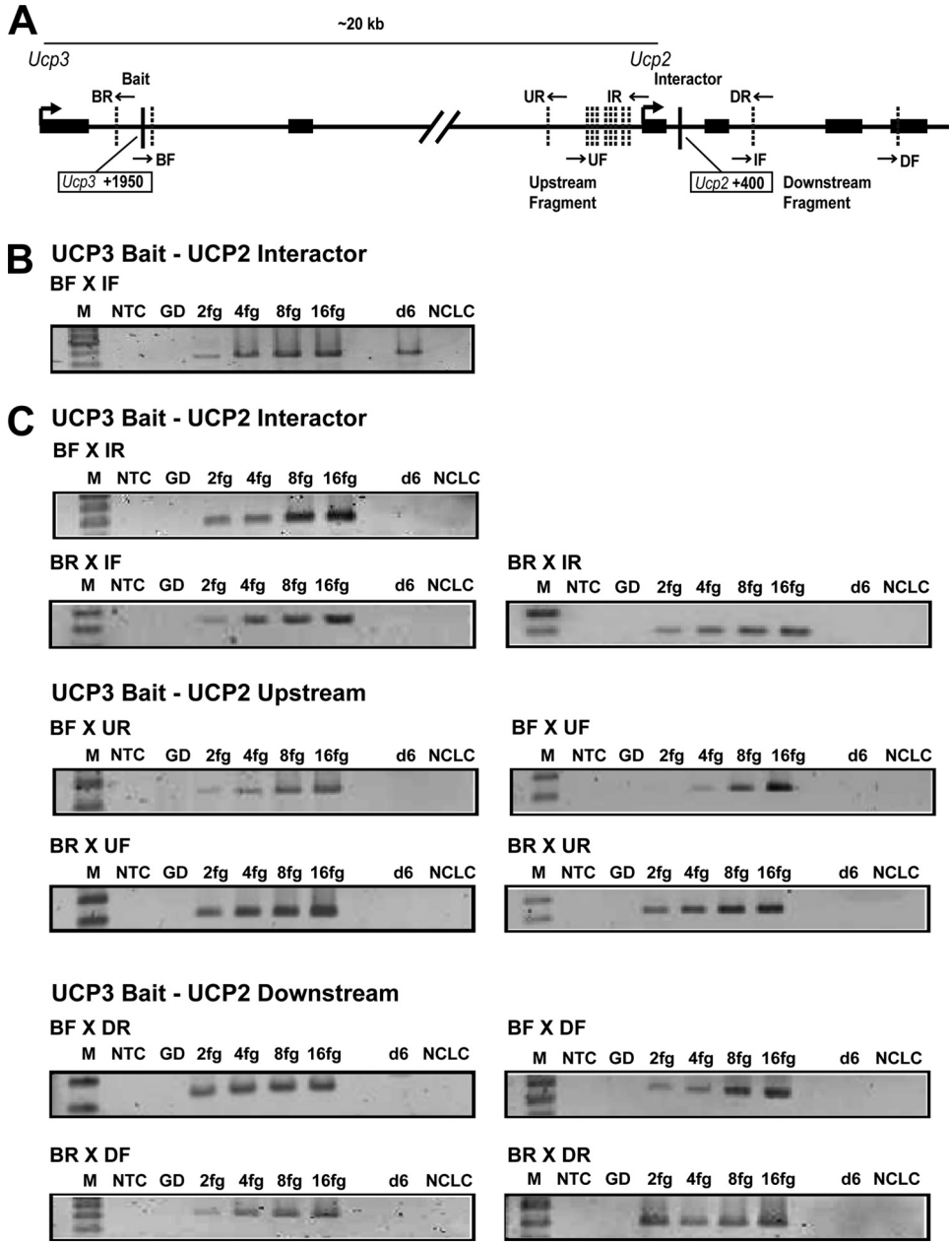

FIGURE 6. **The PPARγ binding site in *Ucp3* intron 1 loops out to specifically interact with the *Ucp2* promoter and 5′-region in adipocytes.** *A*, schematic representation of the mouse *Ucp3* and *-2* loci showing the position of the +1950 and +400 PPARγ/RXR bindings sites in the *Ucp3* and *Ucp2* intron 1, respectively (*solid vertical lines*). Sites recognized by the restriction enzyme Csp6I used in the 3C assay are indicated by *punctuated lines*, and *arrows* mark the positions of the primers used in the 3C analyses. *B*, agarose gel picture showing the 3C PCR amplicons generated with the BF-IF primer combination that detects looping between the bait (restriction fragment covering the +1950 PPARγ/RXR binding site in intron 1 of the *Ucp3* gene) and the interactor (the restriction fragment covering the *Ucp2* promoter and 5′-region, including the +400 PPARγ/RXR bindings site). *C*, agarose gel picture showing the 3C PCR amplicons generated with the indicated primer combinations (see *A*) designed to detect looping between the bait and the genomic regions immediately up- or downstream of the interactor fragment. *Lanes* are as follows: marker (*M*), no template control (*NTC*), Csp6I-digested 3T3-L1 genomic DNA (*GD*), standard curve of control template (*2–16 fg*), 3T3-L1 adipocytes day 6 (*d6*), and non-cross-linked ligated control (*NCLC*).

The PPARγ Binding Site in Ucp3 Intron 1 Interacts with the Ucp2 Gene through DNA Looping—The failure to detect robust binding of PPARγ in the proximity of the *Ucp2* locus was surprising given the many previous observations indicating that the UCP2 gene is a direct target of PPARα and -β/δ in hepatocytes and muscle cells, respectively (16, 18), and of PPARγ in adipocytes (Fig. 1) (28–30). Based on the low intensity of the PPARγ/RXR peak and the finding that the genomic region below the binding site does not contain a DR1 and is unable to mediate PPARγ transactivation of a heterologous promoter, we speculated that this peak might represent a site where PPARγ/RXR interact indirectly with the DNA through other transcription factor complexes recognizing a response element in *Ucp2* intron 1. PPARγ/RXR could be binding indirectly to this site independent of other genomic binding sites, or it could be bound to a PPRE elsewhere in the genome and interact indirectly with the site via long range chromatin interactions. Considering the latter scenario, it is interesting that, in terms of being PPARγ target genes, *Ucp2* and *-3* are quite isolated on chromosome 7 in 3T3-L1 cells with the ChIP-seq data showing >900 and 1400 kb to the next PPARγ/RXR binding site upstream and downstream, respectively (Fig. 2*B*) (40). Thus, the only genomic PPARγ/RXR binding that takes place within reasonable distance of the *Ucp2* gene is at the sites within and upstream of *Ucp3*.

To further investigate the possibility that the PPARγ/RXR-responsive enhancer in intron 1 of the *Ucp3* gene is regulating also the *Ucp2* locus, we employed the 3C technique to determine if these genomic elements engage in specific interactions through DNA looping. 3C is a powerful technique for detecting physical interactions between genomic elements far apart on the same or different chromosomes. In 3C experiments, formaldehyde cross-linked chromatin is subjected to restriction enzyme digestion leading to the formation of discrete complexes containing the DNA strands and interacting proteins that were held in close proximity in the nucleus. The subsequent intramolecular ligation adjoins the neighboring DNA strands in the complex, and these ligation products are then detected by semi-quantitative PCR indicating the interaction frequencies between the chromosomal fragments and thereby the spatial organization of a genomic region. Twelve combinations of eight highly specific primers with comparable sensitivity allowed us to detect all possible intramolecular ligation

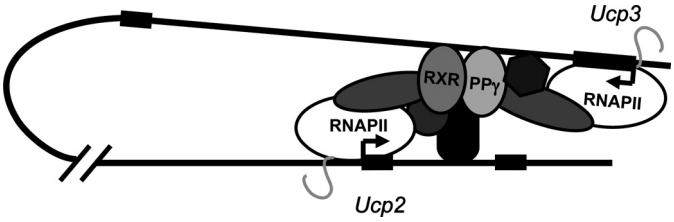

FIGURE 7. **Model for PPARγ transactivation of the UCP3 and -2 genes through intrachromosomal looping.** Our data show that the +1950 PPRE in intron 1 of the *Ucp3* genes is the main PPARγ (*PPγ*) binding site in the *Ucp3* and *-2* loci in murine adipocytes and indicate a model for transactivation of both loci by PPARγ/RXR binding to this PPRE. According to this model PPARγ/RXR bind to the PPRE in intron 1 of the *Ucp3* gene and loop out to simultaneously interact indirectly with intron 1 of the *Ucp2* gene through a transcription factor complex at +400 relative to the transcription start site.

products formed between "the bait," the 850-bp Csp6I restriction fragment containing the PPARγ/RXR binding site in *Ucp3* intron 1, and either "the interactor," the 2450-bp Csp6I restriction fragment covering the *Ucp2* gene from the promoter and into the beginning of intron 2, or the genomic regions immediately upstream and downstream from the interactor (Fig. 6*A*). Interestingly, we found that in 3T3-L1 adipocytes the bait interacts specifically with the interactor (Fig. 6*B*), because no interactions between the bait and the genomic regions immediately up- and downstream of the 2450-bp *Ucp2* fragment was detected (Fig. 6*C*). The fact that only the BF × IF primer combination generated a *Ucp3* bait-*Ucp2* interactor 3C ligation product is indicative of the orientation of the two strands of DNA in the chromatin context. The BR × IR primer set would be expected to generate a product as well in this orientation. The failure to do so is presumably because DNA-bound proteins are obstructing the formation of a fully circular ligation product, a phenomenon often observed in 3C. These results suggest that PPARγ transactivation of both UCP2 and -3 is mediated through the binding site in *Ucp3* intron 1 and DNA looping. A model depicting how this interaction potentially could take place is shown in Fig. 7.

DISCUSSION

UCP2 and -3 are considered *bona fide* PPAR target genes, yet the elements through which this regulation takes place have not been well characterized. We therefore took advantage of our recent ChIP-seq-based mapping of PPARγ and RXR binding during adipocyte differentiation of 3T3-L1 cells (40) to identify potential PPARγ/RXR regulatory elements in the *Ucp2* and *-3* loci. Interestingly, we found the most prominent PPARγ/RXR binding site in the vicinity of the *Ucp3* and *-2* loci to be situated in intron 1 of the *Ucp3* gene at position +1950 relative to the transcription start site. Of the four PPARγ/RXR binding sites found in this region only this intronic site mediated PPARγ transactivation of the heterologous SV40 promoter in luciferase reporter assays (Fig. 4). Importantly, the +1950 binding site in *Ucp3* also enabled PPARγ-mediated transactivation of the cognate endogenous promoter in a manner that was critically dependent on the presence of the DR1 element (Fig. 5*B*). Interestingly, the +1950 DR1 element in *Ucp3* intron 1 is conserved in hamsters and positioned only 30 bp upstream of the single base pair position identified as important for induction of UCP3 expression by PPARγ agonists in brown adipocytes (36).

Surprisingly, we failed to detect any significant binding of PPARγ/RXR to the *Ucp2* locus except from a very low intensity peak in intron 1, which only partially overlapped a degenerated DR1 element at the very edge of the peak (Fig. 2*A*). Moreover, a region of ~500 bp overlapping the peak failed to mediate any PPARγ induction of the SV40 promoter (Fig. 4). Based on these observations we reasoned that the weak PPARγ/RXR binding in *Ucp2* intron 1 could signify indirect interactions of PPARγ/RXR with the DNA mediated through DNA looping. The only detectable genomic PPARγ/RXR binding within the 900-kb distance of the *Ucp2* gene is the binding to the sites within and in the vicinity of the *Ucp3* loci (Fig. 2*B*) (40). Interestingly, using 3C technology we demonstrated that the PPARγ/RXR-responsive enhancer in the *Ucp3* intron 1 indeed loops out to specifically interact with the genomic region stretching from the *Ucp2* promoter and into the second exon in 3T3-L1 adipocytes (Fig. 6, *B* and *C*), where we correspondingly observed PPARγ/RXR binding in intron 1 of the *Ucp2* gene (Fig. 2). The distribution of Csp6I restriction sites in *Ucp2* precludes a better resolution of the exact position of the interaction, but the ChIP-seq and ChIP-PCR data suggest that the *Ucp3* PPRE loops down to a site in intron 1 of *Ucp2*, approximately +400 bp relative to the transcription start site (Fig. 2*A* and Fig. 3). Interestingly, the importance of intron 1 in regulating UCP2 transcription has already been demonstrated by the presence of a silencer element in this region (38). In addition, PPARγ transactivation of UCP2 has been shown to be dependent on the double E-box motif in the proximal promoter (37), but our ChIP-seq data did not provide us with any clues as to why this is the case. The possibility remains that the factors binding to these elements are regulated by the formation and/or stabilization of the intrachromosomal loop between *Ucp2* and *-3*.

In conclusion, we have identified the +1950 PPARγ/RXR binding site in intron 1 of the *Ucp3* gene as the most prominent and functional PPARγ/RXR binding site in the *Ucp3* and *-2* loci. Furthermore, we have shown that this site loops out to specifically interact with the *Ucp2* promoter and 5′-region in adipocytes. Our data indicate that PPARγ/RXR transactivation of both *Ucp2* and *-3* is mediated through the binding site in the *Ucp3* intron 1.

Acknowledgments—We thank R. Ohlsson for vital discussions on the planning and evaluation of the 3C experiments, D. J. Orlicky for the LXSN-hCARΔ1 construct, and P. Sauerberg (Novo Nordisk A/S) for the rosiglitazone/BRL49653 ligand.

REFERENCES

1. Heaton, G. M., Wagenvoord, R. J., Kemp, A., Jr., and Nicholls, D. G. (1978) *Eur. J. Biochem.* **82,** 515–521
2. Cannon, B., and Nedergaard, J. (2004) *Physiol. Rev.* **84,** 277–359
3. Fleury, C., Neverova, M., Collins, S., Raimbault, S., Champigny, O., Levi-Meyrueis, C., Bouillaud, F., Seldin, M. F., Surwit, R. S., Ricquier, D., and Warden, C. H. (1997) *Nat. Genet.* **15,** 269–272
4. Boss, O., Samec, S., Paoloni-Giacobino, A., Rossier, C., Dulloo, A., Seydoux, J., Muzzin, P., and Giacobino, J. P. (1997) *FEBS Lett.* **408,** 39–42
5. Jaburek, M., Varecha, M., Gimeno, R. E., Dembski, M., Jezek, P., Zhang, M., Burn, P., Tartaglia, L. A., and Garlid, K. D. (1999) *J. Biol. Chem.* **274,** 26003–26007
6. Gong, D. W., He, Y., Karas, M., and Reitman, M. (1997) *J. Biol. Chem.* **272,**

24129–24132
7. Arsenijevic, D., Onuma, H., Pecqueur, C., Raimbault, S., Manning, B. S., Miroux, B., Couplan, E., Alves-Guerra, M. C., Goubern, M., Surwit, R., Bouillaud, F., Richard, D., Collins, S., and Ricquier, D. (2000) *Nat. Genet.* **26,** 435–439
8. Gong, D. W., Monemdjou, S., Gavrilova, O., Leon, L. R., Marcus-Samuels, B., Chou, C. J., Everett, C., Kozak, L. P., Li, C., Deng, C., Harper, M. E., and Reitman, M. L. (2000) *J. Biol. Chem.* **275,** 16251–16257
9. Vidal-Puig, A. J., Grujic, D., Zhang, C. Y., Hagen, T., Boss, O., Ido, Y., Szczepanik, A., Wade, J., Mootha, V., Cortright, R., Muoio, D. M., and Lowell, B. B. (2000) *J. Biol. Chem.* **275,** 16258–16266
10. Bouillaud, F. (2009) *Biochim. Biophys. Acta* **1787,** 377–383
11. Pi, J., Bai, Y., Daniel, K. W., Liu, D., Lyght, O., Edelstein, D., Brownlee, M., Corkey, B. E., and Collins, S. (2009) *Endocrinology* **150,** 3040–3048
12. Schrauwen, P., Hoeks, J., Schaart, G., Kornips, E., Binas, B., Van De Vusse, G. J., Van Bilsen, M., Luiken, J. J., Coort, S. L., Glatz, J. F., Saris, W. H., and Hesselink, M. K. (2003) *FASEB J.* **17,** 2272–2274
13. Jucker, B. M., Ren, J., Dufour, S., Cao, X., Previs, S. F., Cadman, K. S., and Shulman, G. I. (2000) *J. Biol. Chem.* **275,** 39279–39286
14. Weigle, D. S., Selfridge, L. E., Schwartz, M. W., Seeley, R. J., Cummings, D. E., Havel, P. J., Kuijper, J. L., and BeltrandelRio, H. (1998) *Diabetes* **47,** 298–302
15. Seifert, E. L., Bézaire, V., Estey, C., and Harper, M. E. (2008) *J. Biol. Chem.* **283,** 25124–25131
16. Nakatani, T., Tsuboyama-Kasaoka, N., Takahashi, M., Miura, S., and Ezaki, O. (2002) *J. Biol. Chem.* **277,** 9562–9569
17. Young, M. E., Patil, S., Ying, J., Depre, C., Ahuja, H. S., Shipley, G. L., Stepkowski, S. M., Davies, P. J., and Taegtmeyer, H. (2001) *FASEB J.* **15,** 833–845
18. Chevillotte, E., Rieusset, J., Roques, M., Desage, M., and Vidal, H. (2001) *J. Biol. Chem.* **276,** 10853–10860
19. Cheng, L., Ding, G., Qin, Q., Huang, Y., Lewis, W., He, N., Evans, R. M., Schneider, M. D., Brako, F. A., Xiao, Y., Chen, Y. E., and Yang, Q. (2004) *Nat. Med.* **10,** 1245–1250
20. Son, C., Hosoda, K., Matsuda, J., Fujikura, J., Yonemitsu, S., Iwakura, H., Masuzaki, H., Ogawa, Y., Hayashi, T., Itoh, H., Nishimura, H., Inoue, G., Yoshimasa, Y., Yamori, Y., and Nakao, K. (2001) *Endocrinology* **142,** 4189–4194
21. Wang, Y. X., Lee, C. H., Tiep, S., Yu, R. T., Ham, J., Kang, H., and Evans, R. M. (2003) *Cell* **113,** 159–170
22. Kersten, S., Desvergne, B., and Wahli, W. (2000) *Nature* **405,** 421–424
23. Nielsen, R., Grøntved, L., Stunnenberg, H. G., and Mandrup, S. (2006) *Mol. Cell. Biol.* **26,** 5698–5714
24. Bugge, A., Grøntved, L., Aagaard, M. M., Borup, R., and Mandrup, S. (2009) *Mol. Endocrinol.* **23,** 794–808
25. Tontonoz, P., Hu, E., and Spiegelman, B. M. (1994) *Cell* **79,** 1147–1156
26. Matsuda, J., Hosoda, K., Itoh, H., Son, C., Doi, K., Hanaoka, I., Inoue, G., Nishimura, H., Yoshimasa, Y., Yamori, Y., Odaka, H., and Nakao, K. (1998) *Diabetes* **47,** 1809–1814
27. Emilsson, V., O'Dowd, J., Wang, S., Liu, Y. L., Sennitt, M., Heyman, R., and Cawthorne, M. A. (2000) *Metabolism* **49,** 1610–1615
28. Camirand, A., Marie, V., Rabelo, R., and Silva, J. E. (1998) *Endocrinology* **139,** 428–431
29. Rieusset, J., Auwerx, J., and Vidal, H. (1999) *Biochem. Biophys. Res. Commun.* **265,** 265–271
30. Aubert, J., Champigny, O., Saint-Marc, P., Negrel, R., Collins, S., Ricquier, D., and Ailhaud, G. (1997) *Biochem. Biophys. Res. Commun.* **238,** 606–611
31. IJpenberg, A., Jeannin, E., Wahli, W., and Desvergne, B. (1997) *J. Biol. Chem.* **272,** 20108–20117
32. Gearing, K. L., Göttlicher, M., Teboul, M., Widmark, E., and Gustafsson, J. A. (1993) *Proc. Natl. Acad. Sci. U.S.A.* **90,** 1440–1444
33. Acín, A., Rodriguez, M., Rique, H., Canet, E., Boutin, J. A., and Galizzi, J. P. (1999) *Biochem. Biophys. Res. Commun.* **258,** 278–283
34. Tu, N., Chen, H., Winnikes, U., Reinert, I., Pirke, K. M., and Lentes, K. U. (2000) *Life Sci.* **67,** 2267–2279
35. Girousse, A., Tavernier, G., Tiraby, C., Lichtenstein, L., Iacovoni, J. S., Mairal, A., Villarroya, F., and Langin, D. (2009) *Diabetologia* **52,** 1638–1646
36. Fromme, T., Hoffmann, C., Nau, K., Rozman, J., Reichwald, K., Utting, M., Platzer, M., and Klingenspor, M. (2009) *Physiol. Genomics* **38,** 54–62
37. Medvedev, A. V., Snedden, S. K., Raimbault, S., Ricquier, D., and Collins, S. (2001) *J. Biol. Chem.* **276,** 10817–10823
38. Yoshitomi, H., Yamazaki, K., and Tanaka, I. (1999) *Biochem. J.* **340,** 397–404
39. Helledie, T., Grøntved, L., Jensen, S. S., Kiilerich, P., Rietveld, L., Albrektsen, T., Boysen, M. S., Nøhr, J., Larsen, L. K., Fleckner, J., Stunnenberg, H. G., Kristiansen, K., and Mandrup, S. (2002) *J. Biol. Chem.* **277,** 26821–26830
40. Nielsen, R., Pedersen, T. A., Hagenbeek, D., Moulos, P., Siersbaek, R., Megens, E., Denissov, S., Børgesen, M., Francoijs, K. J., Mandrup, S., and Stunnenberg, H. G. (2008) *Genes Dev.* **22,** 2953–2967
41. Orlicky, D. J., DeGregori, J., and Schaack, J. (2001) *J. Lipid Res.* **42,** 910–915
42. Hansen, J. B., Petersen, R. K., Larsen, B. M., Bartkova, J., Alsner, J., and Kristiansen, K. (1999) *J. Biol. Chem.* **274,** 2386–2393
43. Helledie, T., Antonius, M., Sorensen, R. V., Hertzel, A. V., Bernlohr, D. A., Kølvraa, S., Kristiansen, K., and Mandrup, S. (2000) *J. Lipid Res.* **41,** 1740–1751
44. Göndör, A., Rougier, C., and Ohlsson, R. (2008) *Nat. Protoc.* **3,** 303–313